

ChemComm

Accepted Manuscript



This is an *Accepted Manuscript*, which has been through the Royal Society of Chemistry peer review process and has been accepted for publication.

Accepted Manuscripts are published online shortly after acceptance, before technical editing, formatting and proof reading. Using this free service, authors can make their results available to the community, in citable form, before we publish the edited article. We will replace this *Accepted Manuscript* with the edited and formatted *Advance Article* as soon as it is available.

You can find more information about *Accepted Manuscripts* in the [Information for Authors](#).

Please note that technical editing may introduce minor changes to the text and/or graphics, which may alter content. The journal's standard [Terms & Conditions](#) and the [Ethical guidelines](#) still apply. In no event shall the Royal Society of Chemistry be held responsible for any errors or omissions in this *Accepted Manuscript* or any consequences arising from the use of any information it contains.

Cite this: DOI: 10.1039/c0xx00000x

www.rsc.org/xxxxxx

ARTICLE TYPE

Side-Functionalized Two-Dimensional Polymers Synthesized via On-Surface Schiff-Base Coupling

Lirong Xu,^a Lili Cao,^a Zongxia Guo,^b Zeqi Zha,^a and Shengbin Lei^{*a}

Received (in XXX, XXX) Xth XXXXXXXXX 20XX, Accepted Xth XXXXXXXXX 20XX

DOI: 10.1039/b000000x

An imine-based 2D polymer side-functionalized with *o*-hydroxyl group was designed in regarding to its potential ability to serve as chelating agents and synthesized on highly oriented pyrolytic graphite surface with relatively low annealing temperature. When annealed to higher temperature the *o*-hydroxyl group reacts further with the imine group, leads to formation of oxazoline, which causes significant distortion to the network. The formation of oxazoline was further confirmed by ATR-FT IR.

Recently, the synthesis and characterization of two-dimensional polymers has attracted significant interest due to its potential application as nanoporous membranes and electronic, photoelectronic materials.¹⁻⁶ Although on-surface synthesis, using a solid surface as template, has been proved to be an efficient approach toward such intriguing materials, the realization of long-range ordered two-dimensional polymer with low defect density still remains a foremost challenge for surface scientists.⁷⁻⁸ Up to now, different types of two-dimensional polymers, or put to another term, surface covalent organic frameworks (surface COFs), based on diverse chemical reactions have been accomplished through on surface synthesis via different reactions.⁹⁻¹⁷ Among all these reactions, the condensation and esterification of boronic acid and Ullmann coupling are most thoroughly investigated. The Schiff-base coupling, which has been widely applied in solution preparation of bulk (powder) COF materials,¹⁸ on the other hand, is less explored in the on-surface synthesis despite the moderate reaction conditions, no need of catalyst and could be prepared on inert surfaces, mostly because the reaction is not easy to proceed in vacuum without catalysis.¹⁹ However, at the solid-liquid interface, Schiff-base reaction can proceed at room temperature.²⁰

Single layer of 2D polymer represents one class of intriguing two-dimensional materials, especially those with 2D π -conjugated structures due to the efficient in-plane electron transport through covalent bond.²¹ These materials bear a finite band gap and can be applied in the field of nanoelectronics as an alternation of graphene,²²⁻²⁴ which is long been boring with its zero band gap nature.^{25,26} The electronic structure of the 2D polymers can be easily engineered by alternating their backbone structure or introducing functional groups onto the backbone.²⁷⁻²⁹ The potential to recognize specific target molecule through the incorporation of tailored recognition sites in a highly organized manner to such molecular scale membrane renders side-functionalization of 2D polymers extremely attractive in nanosensing.²

Introducing functional groups into COF materials by using precursors bearing functional moieties is a straight forward approach and has been successfully realized in bulk COF synthesis.³⁰⁻³³ Though 2D polymers functionalized with side groups have attractive potential applications in chiral separation and nanoelectronics, up to date, on-surface synthesis of 2D polymer with side functional groups is scarce. Introduction of functional groups with chemical activity is especially challenging for the on-surface synthesis due to changes of chemical and physical properties to the monomer and potential side reactions. The only attempt toward side-functionalization of surface COF was reported recently by Faury et al.³⁴ However, side functionalized 2D polymer with long range order and high surface coverage was not obtained.

In this paper, we report on the synthesis of extended 2D polymers with side functional groups and acceptable ordering. The incorporation of hydroxyl groups on the ortho-position equips the 2D polymer with spatially ordered potential chelating sites, attractive in the application of nanosensing and catalysis. We applied a solution based premixing methodology, which impose no limit to the evaporation temperature. 3,3'-Dihydroxybenzidine (DHI) or 3,3'-Dimethoxybiphenyl-4,4'-diamine (DMA), in which the *o*-H of benzidine was replaced with chemical active hydroxy group, or chemical passive methoxy group, were used as precursors to construct functionalized 2D polymers. Both precursors can form regular 2D polymer on highly oriented pyrolytic graphite (HOPG) surface via on-surface Schiff-base coupling with benzene-1,3,5-tricarbaldehyde (BTA).

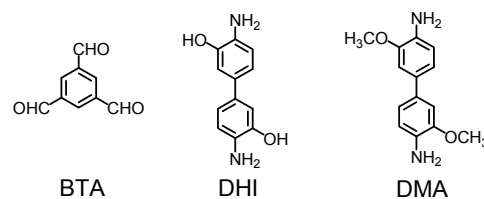


Figure 1. Molecular structure of monomers used in this work.

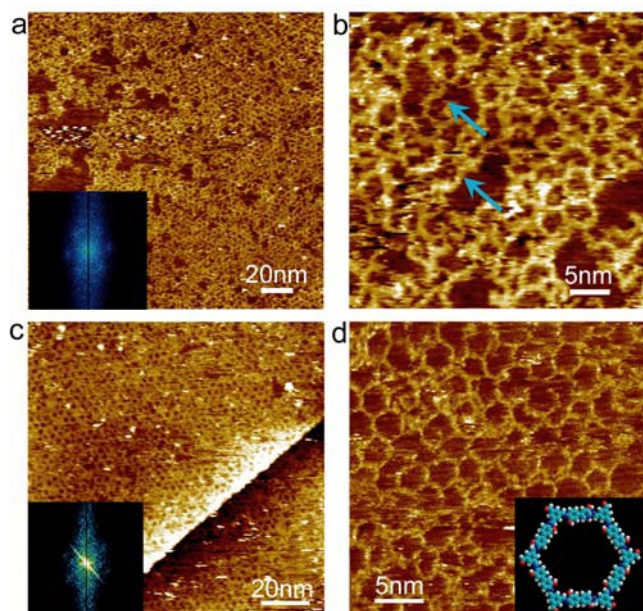


Figure 2. (a) Large-scale STM image of 2DP_{BTA-DHI} obtained by annealing at 65 °C for 30 mins with the corresponding FFT of the STM image inserted. (b) High resolution STM image of the 2DP_{BTA-DHI} shown in (a). Some oligomers resulting from incomplete condensation are indicated by the blue arrows. (c) Large-scale STM image of 2DP_{BTA-DHI} obtained by annealing at 75 °C for 4 hours with the corresponding FFT of the STM image inserted. (d) High resolution STM image of the 2DP_{BTA-DHI} shown in (c). The tunneling conditions were $I_{set} = 0.5$ nA, $V_{bias} = 0.5$ V for (a) and (b), $I_{set} = 0.03$ nA, $V_{bias} = 0.5$ V for (c) and (d).

For the on-surface synthesis of 2DP_{BTA-DHI} on HOPG substrate, BTA and DHI were dissolved in DMSO with a mole ratio of about 1:3 and drop-casted onto the substrate surface. Annealing the sample at 65 °C for 30 min results in an extended network with side functional groups, the two-dimensional fast Fourier transformation (FFT) of the STM image show six scattering spots, indicate the varied periodicity of the network (Figure 2a and inset). High resolution STM image reveals imperfection of the network. Unclosed pores and zig-zag linear polymers from incomplete condensation can be distinguished in the STM image, as indicated by the blue arrows (Figure 2b). After increasing the temperature to 75 °C, the amount of oligomers has significantly decreased (Figure S1). By elongating the reaction time, more extended OH-functionalized 2DP_{BTA-DHI} could be achieved. Figure 2c-d shows representative STM images of 2DP_{BTA-DHI} obtained at 75 °C for 4 hours. The topography of 2DP_{BTA-DHI} is dominated by hexagonal network. The percentage of triple-coordinated vertices increases from 42% for the sample prepared at 65 °C for 30 mins to 65% for the sample prepared at 75 °C for 4 hours, demonstrating a significant increase in the completeness of surface reaction. The lattice parameters of 2DP_{BTA-DHI} were measured to be $a = b = 3.0 \pm 0.2$ nm, $\alpha = 60 \pm 2^\circ$, which agrees well with that expected from the chemical structure, confirming the covalent bond formation.

It is worth noting that annealing the sample at 140 °C for 30 mins results in distorted network topology (Figure S2). As illustrated in Figure 3c, an ideal hexagonal pore formed by Schiff-base coupling of six BTA and six DHI monomer units afford an all *trans*-conformation of imine groups, with the -OH pointing to different sides of the pore. Here *trans*-conformation

refers to the conformation where the two imine bonds point to opposite directions with respect to the molecular axis of DHI (Figure 3a). This motif with uniform bond lengths and ideal 120° bond angles between all sp^2 atoms can serve as building unit for an extended 6-fold symmetric honeycomb framework. However, rotation of single bonds is possible, results in *cis*-conformation of the DHI unit and different orientation of the -OH group. Conformational optimization indicates that the 2DP_{BTA-DHI} can accommodate *cis*-conformation by slightly adjusting the bond angles of the skeleton, and do not lead to significant distortion of the network (Figure S3). This has been proved by the high regularity of the unfunctionalized 2D polymers.²⁹ Intramolecular hydrogen bond between C=N and -OH groups is also possible (Figure 3a), which can enhance the stability of the entire covalent network without changing its geometry. Thus the distortion of the 2D polymer must have other reasons. After complete of the Schiff base reaction, the -OH group can further react with imine, leading to the formation of oxazolidine. In the presence of oxidant (in our case most probably O₂) oxazolidine will further oxidize to oxazoline (Figure 3b). Since there are twelve imine groups in each hexagon, there exist a lot of imine-oxazolidine-oxazoline combinations if the cyclization-oxidation reaction proceeds incompletely. Since the formation of oxazolidine/oxazoline will cause shrinking of the network (Figure 3a), the hybrid network will become distorted. Figure 3b and Figure 3c shows the three-step reaction and chemical models of the Schiff-base product, oxazoline network and some intermediate states with different combinations. The periodicity of the covalent network will decrease to 2.7 nm if all the imine groups completely change to

oxazolines. To get a deeper insight into the relation between reaction temperature and network regularity, we have also tried to proceed the reaction at even higher temperature so that the cyclization/oxidation reaction can be more complete. Annealing at 205 °C for 30 mins leads to a 2D polymer with more distorted pores (Figure 3d and 3e), indicating that more imine groups are converted to oxazolidine/oxazolines. Now the FFT of STM image shows no points, indicating the network completely loss periodicity (Figure S4). Extending the annealing time to 11 hours does not help the imine network completely transfer to oxazoline network (Figure S5). The continuous imine 2DP_{BTA-DHI} network torn apart due to shrinking after cyclization and oxidation.

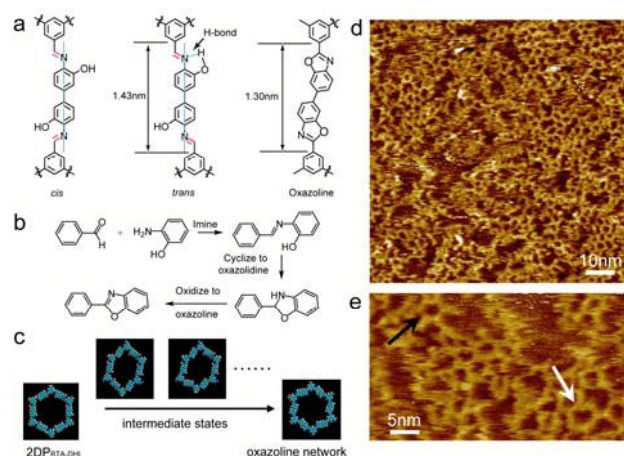


Figure 3. (a) Illustration of the definition of the *cis*- and *trans*-

conformation of imine groups, the formation of intramolecular hydrogen bond, and the structure of oxazoline. (b) Three chemical reaction steps including Schiff-base coupling, cyclization and oxidation of oxazolidine to oxazoline. (c) Structural models of different imine and oxazoline combinations. (d) and (e) Large-scale and high resolution STM image of $2DP_{BTA-DHI}$ obtained after annealing at 205°C for 30 mins. Hexagonal pores supposed to be oxazoline and Schiff-base are indicated by black and white arrows respectively. The tunneling conditions were $I_{\text{set}} = 0.5\text{ nA}$, $V_{\text{bias}} = 0.5\text{ V}$.

To confirm the formation of oxazoline network we have performed total reflection infrared spectroscopy (ATR-FT IR) on the sample prepared at 75°C and 205°C , respectively, as illustrated in Figure S6. In the spectrum obtained on the sample prepared at 75°C the peak at 1650 cm^{-1} is attributed to the vibration of imine $\text{C}=\text{N}$, while for the sample annealed at 205°C , the peak red shift to 1676 cm^{-1} , which is in good agreement with previously reported $\text{N}=\text{C}-\text{O}$ vibration of oxazoline group.⁴⁰⁻⁴¹ The peak at 1170 cm^{-1} is attributed to the vibration of $\text{C}-\text{O}$ bond of the phenol group, appears for both samples, also agrees with the conclusion that not all imine groups were transformed to oxazoline even after annealing at 205°C . It is worth mentioning that we cannot rule out the possible existence of oxazolidine intermediate in the network, since both STM and ATR-FT IR cannot distinguish these two compounds, and also because STM characterization still reveals distorted networks even the reaction was carried out under argon protection (Figure S7).

To further validate the hypothesis we have passivated the chemical active $-\text{OH}$ group by replacing it with $-\text{OCH}_3$. In this case, by using the same preparation procedure, nearly single crystalline $2DP_{BTA-DMA}$ was obtained (Figure 4). The FFT of STM image (the inset of Figure 4a) shows sharp points with 6-fold symmetry. The lattice parameters of this 2D polymer were measured to be $a = b = 3.0 \pm 0.1\text{ nm}$, $\alpha = 60 \pm 2^\circ$, which agrees well with the chemical structure model and confirms the covalent bond formation. Although there are some defects which were indicated by blue arrows in Figure 4a, the orientation and continuity of the $2DP_{BTA-DMA}$ is not affected. The modification by $-\text{OCH}_3$ not only allowed us to accurately adjust the size of the pores (the pore diameter in $2DP_{BTA-DMA}$ decrease to $2.3 \pm 0.1\text{ nm}$) but also change the chemical environment. This result also in one way proved that the distortion in the $-\text{OH}$ functionalized $2DP_{BTA-DHI}$ is due to the further cyclization/oxidation of imine.

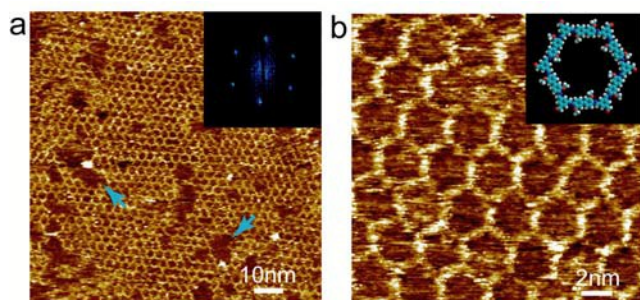


Figure 4. (a) Large-scale STM image of $2DP_{BTA-DMA}$ with the inset depicting the corresponding FFT of the STM image. Structural defects resulted from missing of building blocks are marked by dark blue arrows. (b) High resolution STM image of $2DP_{BTA-DMA}$, the inset shows the chemical structure of a hexagonal pore. The tunneling conditions were $I_{\text{set}} = 0.1\text{ nA}$, $V_{\text{bias}} = 0.5\text{ V}$.

Though the strategy for the side-functionalization of 2D

polymers is straight forward, the implementation is not easy. Chemically active functional groups may result in side reactions which may perturb the network forming reaction. Since post synthetic separation is not possible for the on-surface synthesis of 2D polymers, a small portion of the by-product is enough to lead to significant distortion of the network. Other effects, such as the effect on monomer diffusion and assembling, activity of the main-reaction group, symmetry/topology of the 2D polymer *etc* all should be considered. In our case of solution deposition, the evaporation temperature and thermal stability of the precursors are not as important as for the on-surface synthesis in a UHV system.³⁴ However, the surface mobility and intermolecular interactions between precursors has similar effects on the on-surface polymerization as in UHV. The existence of hydroxyl groups in DHI enables intermolecular hydrogen bonding, the intermolecular interaction becomes much stronger as compared to benzidine and DMA. In our procedure for on-surface polymerization, the amine precursor is always in excess in order to ensure complete reaction of BTA, thus coadsorption of unreacted amine precursors was observed (Figure S1). In case of benzidine and DMA, annealing at 140°C in the low vacuum is enough to remove most of the coadsorbed amine precursors,²⁹ however, in case of DHI, coadsorbed DHI monomers are always observed inside the pores of the 2D polymer, especially those prepared under 65°C and 75°C (Figure S1).

Though in the case of $-\text{OH}$ functionalized $2DP_{BTA-DHI}$ further reaction of $-\text{OH}$ with imine seems inevitable at high temperature, this discovery also have positive aspects. Schiff-base reaction is a well known thermodynamic controlled reversible reaction, and thus the 2D imine polymer is not stable in water, acid or basic environment. However, after cyclization and oxidation the stability of the oxazoline 2D polymer will be greatly improved. Thus this inspired us a new strategy for the synthesis of 2D polymers: first utilizing the self-healing ability of thermodynamic controlled reaction like Schiff-base reaction to form a 2D polymer with periodic lattice, and then stabilize it with a further irreversible reaction to get a 2D polymer with higher stability.

Side-functionalization of 2D polymer with chemically passive groups, like $-\text{CH}_3$ ²⁹ or $-\text{OCH}_3$, is relatively easy to accomplish. The precursors designed with $-\text{CH}_3$ or $-\text{OCH}_3$ as substituents could lead to highly ordered networks. These functional groups could be useful for precisely adjusting the size and chemical environment of the pores.

To summarize, imine based 2D polymers side-functionalized with chemical active $-\text{OH}$ or chemical passive $-\text{OCH}_3$ groups were synthesized via on-surface condensation applying a premixing strategy with mild annealing in a low vacuum oven. STM reveals distortion of the $-\text{OH}$ functionalized $2DP_{BTA-DHI}$ when heated to higher temperature, which is attributed to the further reaction of imine with $-\text{OH}$ group. This hypothesis has been verified by ATR-FT IR characterization. And further by the high regularity of the $2DP_{BTA-DMA}$ after the $-\text{OH}$ group was replaced with passive $-\text{OCH}_3$ group. It is envisaged that the pore size and environment/polarity, even the chemical properties and the band gap of the 2D polymers can be engineered by introducing functional groups into the pore walls and through tuning the polarity of the 2D polymers. However, our results proved that introducing chemically active groups is much more

difficult than chemical passive ones. Nevertheless, the synthesis of extended side functionalized 2D polymers represents a significant step toward the application of this type of facilitating 2D materials. Considering the potential ability of *o*-hydroxyl imine to serve as chelating agents, 2DP_{BTA-DHI} represents a molecular-scale membrane with well-ordered recognition sites toward metal ions, which could be attractive for applications in sensing and catalysis.

This work is supported by the National Science Foundation of China (21173061, 21373070, 21403266), and the Open Project of State Key Laboratory of Robotics and System (HIT) (SKLRS-2015-MS-11). The author also thank Prof. Wujiong Xia for valuable discussion.

Notes and references

^a State Key Laboratory of Robotics and System, Harbin Institute of Technology, Harbin, 150001, People's Republic of China, Fax:0451-86403625, Email: leisb@hit.edu.cn

^b School of Polymer Science and Engineering, Qingdao University of Science and Technology, Qingdao 266042, China

[†] Electronic Supplementary Information (ESI) available: [Extra STM, FFT images of 2D polymers]. See DOI: 10.1039/b000000x/

1. D. F. Perepichka, F. Rosei, *Science*, 2009, **323**, 216-217.
2. N. R. Champness, *Nat. Chem.*, 2014, **6**, 757-759.
3. S. Clair, O. Ourdjini, M. Abel, L. Porte, *Adv. Mater.*, 2012, **24**, 1252-1254.
4. A. M. Brockway, J. Schrier, *J. Phys. Chem. C.*, 2013, **117**, 393-402.
5. S. Blankenburg, M. Bieri, R. Fasel, K. Müllen, C. A. Pignedoli, D. Passerone, *Small*, 2010, **6**, 2266-2271.
6. A. Gourdon, *Angew. Chem. Int. Ed.*, 2008, **47**, 6950-6953.
7. J. W. Colson, W. M. Dichtel, *Nat. Chem.*, 2013, **5**, 453-465.
8. M. Lackinger, W. M. Heckl, *J. Phys. D: Appl. Phys.*, 2011, **44**, 464011-464024.
9. N. A. A. Zwaneveld, R. Pawlak, M. Abel, D. Catalin, D. Gigmès, D. Bertin, L. Porte, *J. Am. Chem. Soc.*, 2008, **130**, 6678-6679.
10. J. F. Dienstmaier, D. D. Medina, M. Dogru, P. Knochel, T. Bein, W. M. Heckl, M. Lackinger, *ACS Nano*, 2012, **6**, 7234-7242.
11. L. Grill, M. Dyer, L. Lafferentz, M. Persson, M. V. Peters, S. Hecht, *Nat. Nanotech.*, 2007, **2**, 687-691.
12. M. Bieri, M. Treier, J. M. Cai, K. Ait-Mansour, P. Ruffieux, O. Gröning, P. Gröning, M. Kastler, R. Rieger, X. L. Feng, K. Müllen, R. Fasel, *Chem. Commun.*, 2009, **45**, 6919-6921.
13. J. C. Russell, M. O. Blunt, J. M. Garfitt, D. J. Scurr, M. Alexander, N. R. Champness, P. H. Beton, *J. Am. Chem. Soc.*, 2011, **133**, 4220-4223.
14. T. Lin, X. S. Shang, J. Adisoejoso, P. N. Liu, N. Lin, *J. Am. Chem. Soc.*, 2013, **135**, 3576-3582.
15. T. Dienel, J. Gómez-Díaz, A. P. Seitsonen, R. Widmer, M. Iannuzzi, K. Radican, H. Sachdev, K. Müllen, J. Hutter, O. Gröning, *ACS nano*, 2014, **8**, 6571-6579.
16. R. Tanoue, R. Higuchi, N. Enoki, Y. Miyasato, S. Uemura, N. Kimizuka, A. Z. Stieg, J. K. Gimzewski, M. Kunitake, *ACS Nano*, 2011, **5**, 3923-3929.
17. X. H. Liu, C. Z. Guan, S. Y. Ding, W. Wang, H. J. Yan, D. Wang, L. J. Wan, *J. Am. Chem. Soc.*, 2013, **135**, 10470-10474.
18. X. Feng, X. S. Ding, D. L. Jiang, *Chem. Soc. Rev.*, 2012, **41**, 6010-6022.
19. S. Weigelt, C. Busse, C. Bombis, M. M. Knudsen, K. V. Gothelf, E. Lægsgaard, F. Besenbacher, T. R. Linderoth, *Angew. Chem. Int. Ed.*, 2008, **47**, 4406-4410.
20. A. Ciesielski, M. E. Garah, S. Haar, P. Kovaříček, Jean-M. Lehn, P. Samori, *Nat. Chem.*, 2014, **6**, 1017-1023.
21. N. R. Champness, *Nat. Nanotech.*, 2007, **2**, 671-672.
22. S. Linden, D. Zhong, A. Timmer, N. Aghdassi, J. H. Franke, H. Zhang, X. Feng, K. Müllen, H. Fuchs, L. Chi, H. Zacharias, *Phys. Rev. Lett.* 2012, **108**, 216801.
23. Y. G. Zhou, Z. G. Wang, P. Yang, X. T. Zu, F. Gao, *J. Mater. Chem.*, 2012, **22**, 16964-16970.
24. M. Abel, S. Clair, O. Ourdjini, M. Mossoyan, L. Porte, *J. Am. Chem. Soc.*, 2011, **133**, 1203-1205.
25. Y. T. Liang, M. C. Hersam, *Macromol. Chem. Phys.*, 2012, **213**, 1091-1100.
26. S. Z. Butler, S. M. Hollen, L. Y. Cao, Y. Cui, J. A. Gupta, H. R. Gutiérrez, T. F. Heinz, S. S. Hong, J. X. Huang, A. F. Ismach, E. Johnston-Halperin, M. Kuno, V. V. Plashnitsa, R. D. Robinson, R. S. Ruoff, S. Salahuddin, J. Shan, L. Shi, M. G. Spencer, M. Terrones, W. Windl, J. E. Goldberger, *ACS Nano*, 2013, **7**, 2898-2926.
27. R. Gutzler, D. F. Perepichka, *J. Am. Chem. Soc.*, 2013, **135**, 16585-16594.
28. P. Zhu, V. Meunier, *J. Chem. Phys.*, 2012, **137**, 244703.
29. L. R. Xu, X. Zhou, Y. X. Yu, W. Q. Tian, J. Ma, S. B. Lei, *ACS Nano*, 2013, **7**, 8066-8073.
30. S. Wan, J. Guo, J. Kim, H. Ihee, D. L. Jiang, *Angew. Chem., Int. Ed.*, 2009, **48**, 5439-5442.
31. C. J. Doonan, D. J. Tranchemontagne, T. G. Glover, J. R. Hunt, O. M. Yaghi, *Nat. Chem.*, 2010, **2**, 235-238.
32. R. W. Tilford, S. J. Mugavero, P. J. Pellechia, J. J. Lavigne, *Adv. Mater.*, 2008, **20**, 2741-2746.
33. L. M. Lanni, R. W. Tilford, M. Bharathy, J. J. Lavigne, *J. Am. Chem. Soc.*, 2011, **133**, 13975-13983.
34. T. Faury, F. Dumur, S. Clair, M. Abel, L. Porte, D. Gigmès, *CrysEngComm.*, 2013, **15**, 2067-2075.
35. M. In't Veld, P. Iavicoli, S. Haq, D. B. Amabilino, R. Raval, *Chem. Commun.*, 2008, 1536-1538.
36. Q. T. Fan, C. C. Wang, L. M. Liu, Y. Han, J. Zhao, J. F. Zhu, J. Kuttner, G. Hilt, M. Gottfried, *J. Phys. Chem. C*, 2011, **118**, 13018-13025.
37. H. Y. Gao, Jörn-H. Franke, H. Wagner, D. Y. Zhong, Philipp-A. Held, A. Studer, H. Fuchs, *J. Phys. Chem. C*, 2013, **117**, 18595-18602.
38. H. T. Zhou, J. Z. Liu, S. X. Du, L. Z. Zhang, G. Li, Y. Zhang, B. Z. Tang, H. J. Gao, *J. Am. Chem. Soc.*, 2014, **136**, 5567-5570.
39. C. H. Schmitz, J. Ikononov, M. Sokolowski, *J. Phys. Chem. C.*, 2011, **115**, 7270-7278.
40. R. H. Lin, J. H. Hsu, *Polym. Int.*, 2001, **50**, 1073-1081.
41. P. Agarwal, M. Choudhary, A. Gupta, P. Tandon, *Vib. Spectrosc.*, 2013, **64**, 134-147.

TOC

An imine-based 2D polymer side-functionalized with *o*-hydroxyl group was design and synthesized on highly oriented pyrolytic graphite surface.

5

